PHYSICAL REVIEW A VOLUME 8, NUMBER 6 DECEMBER 1973

Decay of Krypton $1s_2$ and $1s_3$ Excited Species in the Late Afterglow*

R. T. Ku,† J. T. Verdeyen, B. E. Cherrington, and J. G. Eden
Gaseous Electronics Laboratory, Department of Electrical Engineering, University of Illinois at Urbana-Champaign, Urbana, Illinois 61801

(Received 23 April 1973; revised manuscript received 7 August 1973)

Experimental investigations of the behavior of the Kr $1s_2$ excited-state population in afterglow discharge plasmas are described. The number density of Kr $1s_2$ atoms was obtained by performing resonant absorption measurements at 8509 Å (Kr $1s_2 \rightarrow 2p_4$) with a tunable GaAs laser diode. The narrow-width laser was tuned and swept through the entire resonant transition. The decay of the $1s_2$ species in the late afterglow was found to depend primarily on the decay processes for the $1s_3$ species. Analysis of the pressure-dependent decay curve in the late afterglow has been carried out to derive the diffusion coefficient as well as two-body and three-body destruction frequencies for Kr $1s_3$ excited species. The diffusion coefficient was found to be 49 cm^2s^{-1}. The two-body collisional destruction rate was found to be 9×10^{-15} cm^3/s. The three-body collisional destruction rate, which presumably indicates the rate of formation of the excited dimer Kr_2^*, was found to be 53.6×10^{-33} cm^6/s.

I. INTRODUCTION

Studies of the general behavior of excited-state species in afterglow discharges originated with the lifetime measurements of Meissner[1] and Dorgelo.[2] Their experiments were performed by transmitting a beam of light through an absorption tube at various times after the excitation in the tube had been cut off. They called the length of time beyond which absorption was not perceptible the lifetime of the excited-state species. The pressure dependence of the lifetime was then related to the destruction processes of the excited species in the afterglow.

The absorption techniques for the lifetime measurement have been modernized since then by many experiments,[3-9] and recent measurements have been made for the metastable species ($1s_5$ and $1s_3$) and resonant species ($1s_2$ and $1s_4$) in noble-gas afterglow discharges. For example, Phelps[3,4] and Molnar[4] have used the absorption technique to study the Ne $1s_{2-5}$ species as well as the helium $2\,^3S$ and argon $1s_5$ excited species. Ellis and Twiddy[9] have also studied the argon excited species. Lifetimes for the Kr $1s_4$ and $1s_5$ excited atoms have been measured by Smith and Turner,[7,8] and their results were interpreted by assuming the dominant destruction processes to be diffusion to the tube wall (for metastables), radiative decay to the ground state (for the resonant species), plus collisional transfers among $1s_{2-5}$ species. Diffusion coefficients, excitation or deexcitation frequencies, and cross sections for these processes were successfully obtained from the above experiments.

In this paper we report the measurement of the density of krypton $1s_2$ excited species as a function of time in afterglow discharges. These experiments were performed over the pressure range 0.1–25 torr. The variation of the lifetime of the excited species with pressure has been used to determine the two- and three-body collisional destruction rates as well as the diffusion coefficients.

In Sec. II we describe the experimental apparatus, techniques, and typical data. In Sec. III we discuss the important destruction processes for the Kr $1s_2$ and $1s_3$ excited species and develop the theoretical basis on which to interpret the experimental data. In Sec. IV the calculated rate coefficients are presented and are compared with both experimental and theoretical values for previously studied noble-gas excited species.

II. EXPERIMENTAL APPARATUS AND TECHNIQUES

The experimental setup used for the resonant absorption measurements in Kr afterglow plasmas is shown in Fig. 1 and is similar to that used earlier for studies of Cs vapor and Ar active discharges.[10] The radiation source was provided by a tunable GaAs laser operating at 77°K and the radiation was collimated and propagated through an absorption tube 30 cm long and 1 cm inside diam. The transmitted output from one particular laser mode was selected by using a monochromator with 1-Å resolution in front of the photomultiplier. A dc current was applied to coarse tune the laser-mode wavelength to the approximate range of the resonant radiation, 8509 Å ($1s_2 \rightarrow 2p_4$) in the Kr case. Precise frequency matching was achieved by applying long current pulses to the laser (>100 μs) to sweep or "chirp" through the entire Kr absorption line. The laser can be considered

as a δ-function intensity source as it sweeps through the transition due to its narrow frequency width (<1 MHz).

As can be seen from Fig. 1, the laser was pulsed on for approximately 200 μs at a 60-cycle repetition rate. The krypton discharge was produced at a 30-cycle rate (every second laser pulse) by pulsing the discharge on for approximately 30 μs. The discharge current was variable over a range of 0.6–2.6 A. Due to the short discharge pulse and long interval between pulses, the average energy deposited in the gas was quite low and the gas temperature was taken to be 300°K.

In order to measure the absorption of the laser radiation as a function of time in the krypton afterglow, the timing of the discharge pulse could be adjusted so that the laser radiation swept through line center at any given time in the afterglow. Therefore, by measuring the absorption of the laser radiation at line center at various times in the afterglow, accurate measurements of the decay of the Kr $1s_2$ species in the afterglow were obtained. Figure 2 shows some typical oscilloscope displays of the raw data. In Fig. 2(a) the discharge current was pulsed on at the same time that the laser was sweeping through line center, $t = t_0$. The high density of Kr $1s_2$ excited species in the discharge easily caused an ~100% absorption of the laser emission at line center, as can be seen in the upper trace. In Fig. 2(b) the timing was changed so that the discharge pulse occurred at a time t before the laser was swept through line center. The decreased absorption of the laser emission is indicative of the Kr $1s_2$ density at a time t in the afterglow.

Also shown on this figure is the "boxcar gate." In order to obtain accurate and sensitive measurements into the late afterglow, the laser emission was sampled during the time of the boxcar gate shown and the signal was stored by a boxcar integrator. Since the boxcar gate operated at a 60-cycle rate, the boxcar integrator would sample and store the full laser output on one sample and then it would sample and store the laser signal attenuated by the krypton $1s_2$ species on the next sample. The ac component of the boxcar output was then a measure of the amount of laser light absorbed, or the density of the Kr $1s_2$ species, and could be accurately read by a phase-sensitive detector.

Once the attenuation of the laser signal over the cell path length is known, then the absorption constant $k_t(\nu_0)$ can be calculated and the Kr $1s_2$ species density N found from the relationship[11]

$$k_t(\nu_0) = \frac{2}{\Delta\nu_D}\left(\frac{\ln 2}{\pi}\right)^{1/2}\frac{\lambda_0^2}{8\pi}\frac{g_2}{g_1}NA,$$

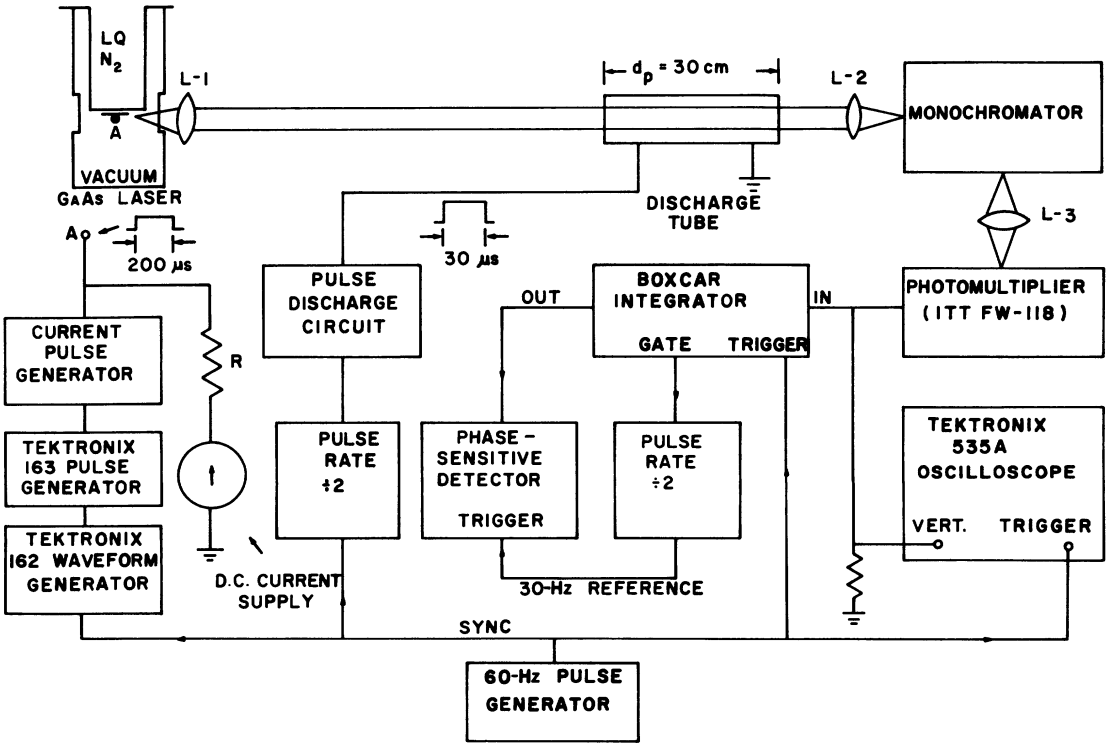

FIG. 1. Experimental apparatus.

where we have assumed a Doppler-broadened profile of width $\Delta\nu_D$; g_2 and g_1 are statistical weights and A is the Einstein coefficient.

Using this technique, the density of Kr $1s_2$ excited atoms was measured in our experimental apparatus as a function of time in the afterglow and as a function of Kr pressure and pulsed discharge current. An example of the density measurements taken in 1.5-torr Kr is shown in Fig. 3. At the lower discharge currents the Kr $1s_2$ decay rate is independent of current and can be characterized by a single time constant β, which is dependent upon the pressure. This is in contrast to the results of Turner,[8] who found a current-independent fast decay (in the early afterglow), as well as the slow decay in late afterglow. Figure 4 shows the dependence of β upon pressure. It is found that the pressure dependence of β can be accurately represented by the empirical relation

$$\beta = (1250/P) + 320P + 68P^2,$$

where β is in s^{-1} and P is in torr.

In Sec. III the time constant β and its pressure dependence will be interpreted in terms of the fundamental destruction processes in the afterglow.

III. THEORY

A. 1s Configuration

Figure 5 presents partial energy-level diagrams for the metastable and resonant excited species in neon, argon, and krypton. There is an obvious similarity among the three gases, where the $1s$ species consist of two metastable species ($1s_3$, $1s_5$) with long natural lifetimes (>1.0 s)[12] and two resonant species ($1s_2$, $1s_4$) with very short natural lifetimes (~10^{-9} s) but long effective lifetimes (~10^{-6} s) due to the trapping of the resonance radiation.[13,14]

In considering the decay of the $1s$ species, particular attention must be paid to the collisional mixing, or excitation transfer, among the $1s$ species. Because the collisional mixing effects depend on the energy discrepancies, we should expect the closest couplings for the $1s$ levels to be found in neon and the least in krypton (see Fig. 5). This was shown experimentally by Phelps[3] for the neon case, where four coupled rate equations had to be solved to separate the mixing effects. For example, the decay rate of the neon $1s_3$ species in the afterglow depends upon its own diffusion rate, and also upon the deexcitation rates to $1s_5$ and $1s_4$ species plus an excitation rate from the $1s_2$ species.

The largest energy separations between the $1s$ states are found in the krypton. In fact, Turner[8] has shown that they can be separated into two groups according to the energy differences. The lower group consists of the $1s_4$ and $1s_5$ levels, and they are separated by 0.117 eV. The upper group consists of the $1s_2$ and $1s_3$ levels, and they are separated by 0.081 eV. The two groups are themselves set apart by a large energy difference of 0.53 eV.

B. Destruction Processes in Kr Afterglow

We will now list some of the more probable destruction mechanisms for excited atoms in the krypton afterglow. Each of these mechanisms will then be discussed to identify its role in the destruction of Kr $1s_2$ and $1s_3$ excited atoms.

We have (i) two-body collisions with one neutral atom resulting in excitation transfer between excited species. (ii) Three-body collisions with two neutral atoms resulting in the deexcitation of the excited species. This primarily occurs through the formation of an excited molecule, which subsequently decays and dissociates to form two ground-state neutral atoms. (iii) Emission of resonance radiation ($1s_2$) which escapes to the wall. (iv) Diffusion of the metastables ($1s_3$) to the wall. (v) Superelastic collisions between excited

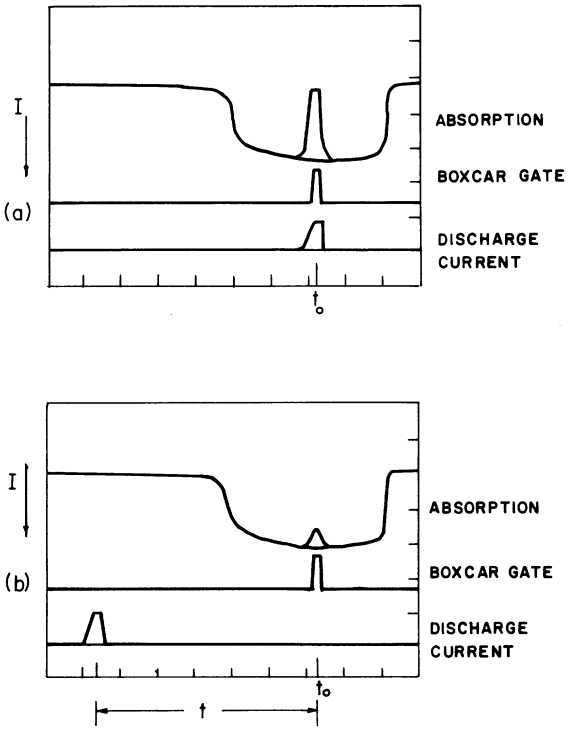

FIG. 2. Typical oscilloscope waveforms for resonant absorption experiments at 8509 Å in Kr afterglows. (a) Plasma is pulsed on at t_0 when the laser is at line center. (b) Plasma is pulsed on at time t before t_0. Time scale = 50 μs/division.

atoms and electrons in the afterglow. (vi) Collisions between excited atoms and other excited atoms, resulting in the ionization of one atom and the deexcitation of the other. (vii) Collisions between excited atoms and foreign-gas atoms.

First of all, we wish to show that processes (v)–(vii) can be neglected under the conditions of this experiment.

(v) Our justification for the neglect of superelastic collisions can be seen in Fig. 3. If we do have a significant contribution from superelastic collisions, the decay should not be exponential in time and the decay rate should depend on the discharge current. In our experiments it has been found that the decay of the $1s_2$ resonant species in the later afterglow is independent of current and is exponential over several orders of magnitude. In fact, the only evidence of current-dependent effects is seen in Fig. 3 for a discharge current of 2.6 A in the very early afterglow ($<200\ \mu$s). At lower currents in the early afterglow and for all currents in the late afterglow no current dependence was found, and so process (v) can be neglected.

(vi) We may also invoke this current independence of the decay rate as a strong argument in favor of neglecting excited-atom collisions. Certainly the density of excited atoms increases with increasing current, as shown in Fig. 3. Therefore, the effect of excited-atom–excited-atom collisions should be seen in a nonexponential decay and in an increased decay rate at higher discharge currents if process (vi) plays an important role. This effect was not observed. The neglect of excited-atom–excited-atom collisions also seems reasonable on the grounds that the metastable density is typically on the order of 10^{-7}–10^{-8} of the neutral-gas density, as can be verified by examining Fig. 3, where the neutral-gas density is $\sim 5\times10^{16}$ cm^{-3}.

(vii) The major impurity in the krypton used in these experiments is 25 ppm of xenon, as contained in the research-grade gas. The vacuum system had a base pressure of $\sim 10^{-7}$ torr, and the

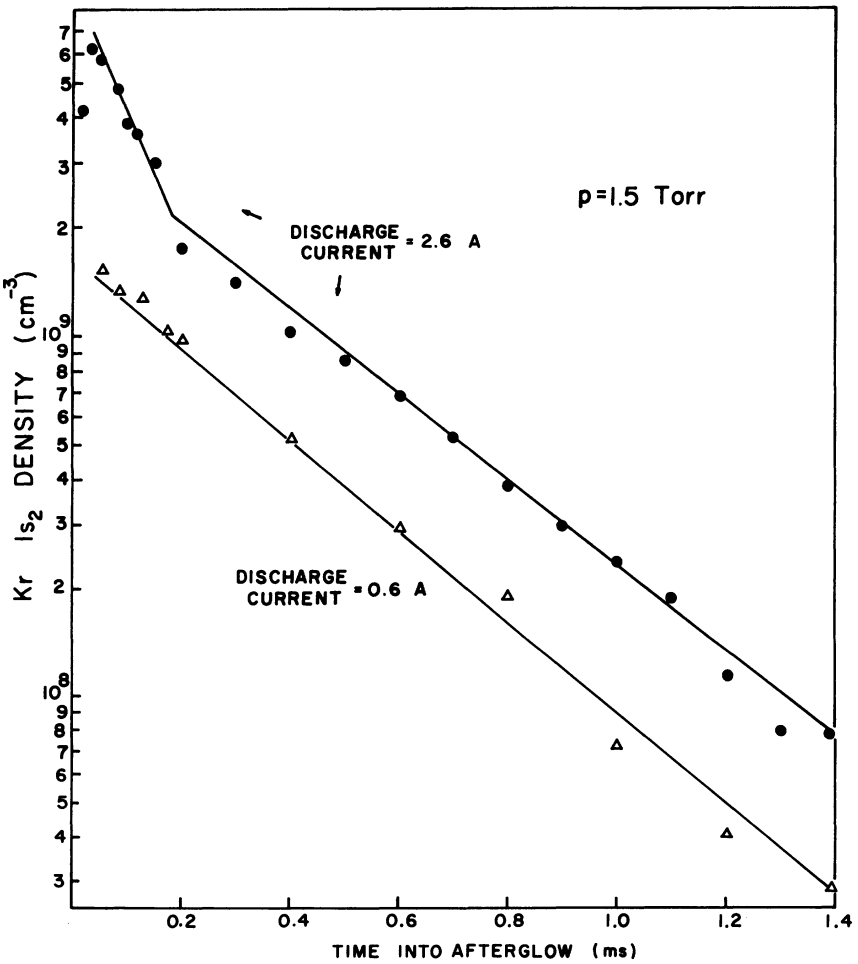

FIG. 3. Measured values of the absolute densities of Kr $1s_2$ excited species as a function of time following a pulsed discharge.

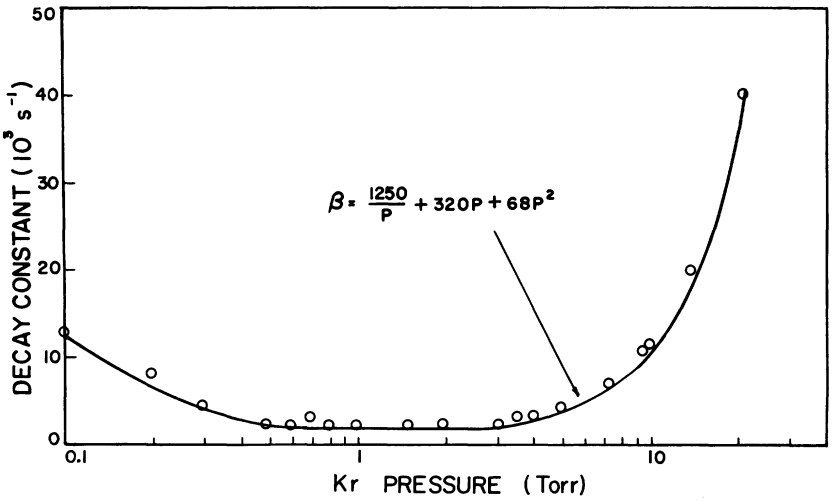

FIG. 4. Measured decay frequencies for Kr $1s_2$ excited species as a function of Kr pressure. Solid line represents an empirical decay curve as a function of pressure.

krypton bottle was attached to a barium getter, so no other significant impurities were present in the system. Since the total impurity level is low, it is expected that excited-atom–impurity collisions did not play an important role in the Kr $1s_2$, $1s_3$ deexcitation.

Consequently, processes (i)–(iv) will be considered as the only major destruction mechanisms for the $1s_2$ ans $1s_3$ excited species. Each of these processes will now be discussed in more detail.

(i) Two-body collisions can result in either the further excitation or the deexcitation of an excited atom. However, two-body collisions are important only when the energy discrepancy between initial and final states is small. For excitational collisions, an energy gap $>> kT$ makes such collisions unlikely. Similarly, for deexcitational collisions, the law of excitation transfer[15] states that the cross section for deexcitation decreases as the energy discrepancy between initial and final states increases. For these reasons, collision-induced transitions between the upper pair of levels ($1s_2$, $1s_3$) and the lower pair of levels ($1s_4$, $1s_5$) are assumed to be negligible compared to the excitation and deexcitation collisions (collisional mixing) occurring between the $1s_2$ and $1s_3$ excited states.[8] Similarly, two-body collisional deexcitation to ground is ignored.

(ii) Three-body collisions have been found to be a strong destruction process for the lower metastable ($1s_5$) level in krypton by Turner,[8] and in Ne, Ar, and Xe by other workers.[4,16] In krypton the deexcitation of the $1s_3$ state results in the formation of an excited dimer[16]:

$$Kr^M + 2Kr \rightarrow Kr_2^* + Kr + E_K ,$$

where E_K is the kinetic energy. Subsequently, the excited molecule dissociates, emitting a nonresonant uv photon:

$$Kr_2^* \rightarrow 2Kr + h\nu .$$

This two-step, three-body process makes it possible to conserve energy and momentum in the deexcitation of the $1s_2$ and $1s_3$ species to ground.

(iii) The resonance ($1s_2$) species has a very short natural lifetime ($\tau_N \sim 10^{-9}$ s).[8] However, because the 1165-Å radiation is heavily trapped, the species is then characterized by an effective lifetime (assuming the resonance line to be pressure broadened) τ_R, given by[13,14]

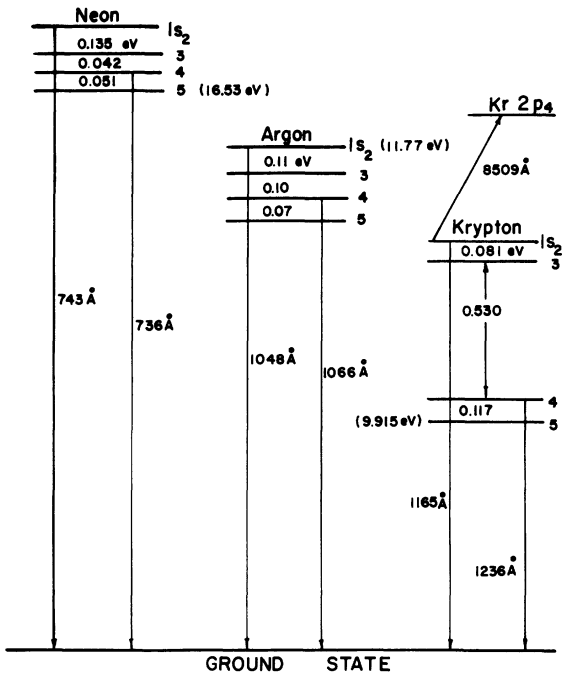

FIG. 5. Partial energy diagram of neon, argon, and krypton 1s levels.

$$(1/\tau_R) = (1/\tau_N)[0.205(\lambda/R)^{1/2}] \simeq 10^6\ \mathrm{s}^{-1},$$

where

$$\lambda = 1165\ \text{Å}\quad (1s_2 \rightarrow \text{ground})$$

and R is radius of the discharge tube, equal to 0.5 cm.

(iv) Diffusion of the metastable ($1s_3$) species to the discharge-tube walls will be characterized by the decay rate D_M/Λ^2, where $\Lambda^2 = [(\pi/L)^2 + (2.4/R)^2]^{-1}$ (assuming the fundamental diffusion mode is dominant in the late afterglow). Λ has units of cm, and D_M, the diffusion coefficient, has units of $\mathrm{cm}^2\ \mathrm{s}^{-1}$. L is the length of the discharge tube.

The dominant decay processes are shown schematically in Fig. 6, where $\gamma_R N^2$, $\gamma_M N^2$ represent the three-body $1s_2$, $1s_3$ destruction rates, respectively; $\alpha_{RM}N$, $\alpha_{MR}N$ represent the two-body destruction rates for the $1s_2$, $1s_3$ excited species, and R, M, and N represent the resonance ($1s_2$), metastable ($1s_3$), and neutral ground-state densities, respectively.

C. Rate Equations

Using Fig. 6, the rate equations governing the time dependence of the resonance ($1s_2$) and metastable ($1s_3$) populations are

$$\frac{dR}{dt} = -\left(\frac{1}{\tau_R} + \alpha_{RM}N + \gamma_R N^2\right) R + \alpha_{MR} NM \qquad (1)$$

and

$$\frac{dM}{dt} = -\left(\frac{D_M}{\Lambda^2} + \alpha_{MR}N + \gamma_M N^2\right) M + \alpha_{RM} NR. \qquad (2)$$

Note that because of the large energy separation between the upper pair ($1s_2$, $1s_3$) and the lower pair ($1s_4$, $1s_5$) of energy levels, we have been able to represent the excited-state populations by two coupled rate equations rather than four, as used by Phelps for neon. This is similar to what Turner was able to do for the $1s_4$, $1s_5$ levels of krypton.

The solution to (1) is of the form

$$R = Ae^{-t/\tau_1} + Be^{-t/\tau_2}, \qquad (3)$$

where A and B are constants and τ_1 and τ_2 are solutions of the quadratic equation

$$\tau_{1,2}^{-1} = \tfrac{1}{2}[-(\alpha+\beta) \pm (\alpha-\beta)]\,\{1 + [4\xi\Delta/(\alpha-\beta)^2]\}^{1/2}, \qquad (4)$$

where

$$\alpha = (1/\tau_R) + \alpha_{RM}N + \gamma_R N^2,$$

$$\beta = (D_M/\Lambda^2) + \alpha_{MR}N + \gamma_M N^2,$$

$$\xi = \alpha_{MR}N, \quad \Delta = \alpha_{RM}N.$$

Under the assumption (see Appendix) that

$$4\xi\Delta \ll (\alpha-\beta)^2,$$

Eq. (3) becomes

$$R = Ae^{-\alpha t} + Be^{-\beta t}. \qquad (5)$$

From the definitions of α and β given earlier and assuming $\alpha > \beta$ (which will be verified in the Appendix) the decay of the resonance species population is dominated by the second term of (5) for times in the late afterglow. Thus, for the late afterglow (which we are investigating here),

$$R \simeq Be^{-\beta t}. \qquad (6)$$

It is interesting to note that the dominant decay rate of the *resonant* species in the late afterglow is dependent on the diffusion coefficient and the two- and three-body destruction frequencies for the *metastable* state. Therefore it appears that the primary source of $1s_2$ excited atoms in the late afterglow is by collisional conversion of the $1s_3$ species.

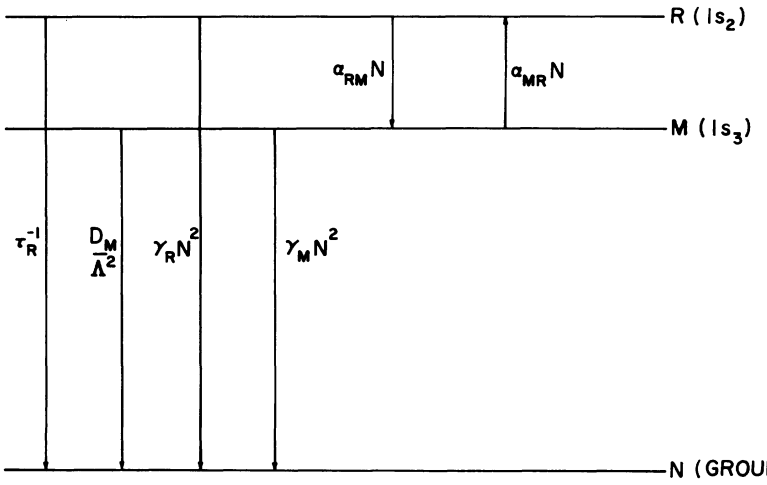

FIG. 6. Schematic diagram of the Kr $1s_2$, $1s_3$ destruction processes.

IV. ANALYSIS OF DATA

From Sec. III, β was found to depend on the metastable diffusion coefficient and two-body and three-body destruction frequencies in the following way:

$$\beta = (D_M/\Lambda^2) + \alpha_{MR} N + \gamma_M N^2.$$

The above relation can be easily changed to a pressure dependence yielding

$$\beta = (D_0/P)(1/\Lambda^2) + \alpha_{MR}(N_0 P) + \gamma_M (N_0 P)^2, \quad (7)$$

where D_0 is the diffusion coefficient at 1 torr (reduced to 0°C), $N_0 = 3.56\times10^{16}$ cm^{-3} is the neutral-gas density at 1 torr and 300°K, and P is the gas pressure in torr.

We see that Eq. (7) has the same functional dependence as our experimentally derived relationship

$$\beta = (1250/P) + 320P + 68P^2. \quad (8)$$

Comparing Eqs. (7) and (8), we can solve for the parameters D_0, α_{MR}, and γ_M.

The results are D_0, the diffusion coefficient at 1 torr (reduced to 0°C) and 300°K, equals 49 cm^2 s^{-1}; α_{MR} is the two-body $1s_3$ metastable destruction frequency, which is equal to 9.0×10^{-15} cm^3 s^{-1}; and γ_M is the three-body destruction frequency (conversion to the excited dimer Kr_2^*), which is equal to 53.6×10^{-33} cm^6 s^{-1}. These results, along with similar parameters for the excited states in other noble gases, are presented in Table I. It is clear that our results are in good agreement with those of Turner for the $1s_5$ level and follow the general trend of decreasing diffusion coefficient and increasing three-body deexcitation as we go from the lighter to the heavier rare gases. Note, however, that three-body collisions, which are of particular importance to krypton, appear to be more important in the destruction of the $1s_3$ metastables than for the $1s_5$ metastables.

Little work has been done previously on the $1s_2$ and $1s_3$ levels in krypton, so it is difficult to compare our results with those of previous investigators. Bouciqué and Mortimer[16] have published a value of 44×10^{-33} cm^6 s^{-1} as the three-body destruction frequency for krypton (as compared to our value of 53.6×10^{-33} cm^6 s^{-1}), but they do not state which metastable level they are referring to, $1s_3$ or $1s_5$. Their data for the three-body collisional destruction frequency for argon show a similar discrepancy, being lower than other reported measurements.

In conclusion, our results for the diffusion coefficient and for the two- and three-body destruction rates are consistent with the results of previous investigations of the properties of excited species in rare gases. The large three-body collisional destruction rate is of particular significance, in that the three-body collisions are responsible for the formation of the excited dimer Kr_2^*, which is the source of nonresonant uv radiation. This large conversion rate suggests that high-pressure krypton discharges would be good candidates for possible molecular-dissociation lasers.

ACKNOWLEDGMENTS

We are grateful to Dr. J. Marinace of IBM Thomas Watson Research Laboratory and Dr. J. Ripper of Bell Telephone Laboratories for providing the cw GaAs lasers for this project. We also appreciate the valuable consultations with Professor Nick Holonyak on the subject of semiconductor lasers, and the general inspiration and encouragement of Professor L. Goldstein.

APPENDIX

Here we wish to show that

$$4\xi\Delta \ll (\alpha - \beta)^2. \quad (A1)$$

From the definitions given earlier we have

$$4\xi\Delta = 4\alpha_{MR}\alpha_{RM}N^2 \quad (A2)$$

TABLE I. Average diffusion constants and two- and three-body destruction rates for noble-gas excited species (300 °K).

Excited species	Reference	Two-body destruction rate (cm^3/s)	Three-body rate (cm^6/s)	Diffusion constant (cm^2/s)
He 2^3S	3	...	0.25×10^{-33}	470
Ne $1s_5$	3	...	0.5×10^{-33}	139
Ne $1s_3$	3	8.0×10^{-15}	...	152
Ar $1s_5$	9	0.7×10^{-15}	17×10^{-33}	44
Ar $1s_3$	9	4.0×10^{-15}	11.4×10^{-33}	47
Kr $1s_5$	7	2.2×10^{-15}	38×10^{-33}	30
Kr $1s_3$	This work	9.0×10^{-15}	53.6×10^{-33}	49

and

$$(\alpha-\beta)^2=\left(\frac{1}{\tau_R}+\gamma_R N^2+\alpha_{RM}N - \frac{D_M}{\Lambda^2}-\gamma_M N^2-\alpha_{MR}N\right)^2.$$

Now, once α_{MR} is known, α_{RM} is determined from the relation for detailed balance:

$$\frac{\alpha_{MR}}{\alpha_{RM}}=\frac{2J_R+1}{2J_M+1}\exp\left(\frac{-(E_R-E_M)}{kT}\right)$$
$$=2.22\times10^{-2} \text{ at } 300^\circ\text{K}.$$

Hence

$$4\xi\Delta\simeq 2\alpha_{MR}^2 N^2\times10^2\sim2\times10^7.$$

Using the values calculated earlier for the diffusion coefficient and the two- and three-body destruction frequencies, we see that $1/\tau_R$ dominates the term $(\alpha-\beta)$. (Incidentally, this also supports our previous assertion that $\alpha>\beta$.) Hence

$$(\alpha-\beta)^2\sim10^{12}>>4\xi\Delta\sim2\times10^7;$$

so our previous assumption is valid.

---

*Work sponsored by the National Science Foundation under Grant No. NSF-GK-27759 and by the Physical Electronics Affiliates Program at the University of Illinois. This paper is based in part upon a dissertation submitted by R. T. Ku to the University of Illinois in partial fulfillment of the requirements for the degree of Ph.D.

†Present address: MIT Lincoln Lab., Lexington, Mass.

[1]W. Meissner, Ann. Phys. (Leipz.) 76, 124 (1925).
[2]H. B. Dorgelo, Z. Phys. 34, 766 (1925).
[3]A. V. Phelps, Phys. Rev. 114, 1011 (1959); Phys. Rev. 99, 1305 (1955).
[4]A. V. Phelps and J. P. Molnar, Phys. Rev. 89, 1202 (1953).
[5]D. J. Eckl, Can. J. Phys. 31, 804 (1952).
[6]J. R. Dixon and F. A. Grant, Phys. Rev. 107, 118 (1957).
[7]D. S. Smith and R. Turner, Can. J. Phys. 41, 1949 (1963).
[8]R. Turner, Phys. Rev. 140, A426 (1966).
[9]E. Ellis and N. D. Twiddy, J. Phys. B 12, 1366 (1969).
[10]R. T. Ku, J. T. Verdeyen, B. E. Cherrington, and L. Goldstein, J. Appl. Phys. 43, 4579 (1972).
[11]A. C. G. Mitchell and M. W. Zemansky, *Resonance Radiation and Excited Atoms* (Cambridge U. P., Cambridge, England, 1934).
[12]R. S. Van Dyck, Jr., C. E. Johnson, and H. A. Shugart, Phys. Rev. A 5, 991 (1972).
[13]T. Holstein, Phys. Rev. 72, 1212 (1947).
[14]T. Holstein, Phys. Rev. 83, 1159 (1953).
[15]H. S. W. Massey and E. H. S. Burhop, *Electronic and Ionic Impact Phenomena* (Oxford U. P., London, 1952), Chap. VII, Sec. 10.
[16]R. Boucique and P. Mortimer, J. Phys. D 3, 1905 (1970).